Pressure-induced quantum phase transitions in the $S = \frac{1}{2}$ triangular lattice antiferromagnet $CsCuCl_3$

A. Sera,[1] Y. Kousaka,[2,3] J. Akimitsu,[2,3] M. Sera,[4] and K. Inoue[1,3,5]

[1]*Graduate School of Science, Hiroshima University, Higashi-Hiroshima 739-8526, Japan*

[2]*Research Institute for Interdisciplinary Science, Okayama University, Okayama 700-8530, Japan*

[3]*Center for Chiral Science, Hiroshima University, Higashi-Hiroshima 739-8526, Japan*

[4]*Department of ADSM, Hiroshima University, Higashi-Hiroshima 739-8530, Japan*

[5]*IAMR, Hiroshima University, Higashi-Hiroshima 739-8526, Japan*

(Received 13 April 2017; revised manuscript received 19 June 2017; published 14 July 2017)

We investigated the pressure effect on the magnetization of the soft material $CsCuCl_3$. We also measured the lattice distortion under the longitudinal magnetic fields at the ambient pressure. While the *ab* plane shrinks in all the quantum phases below T_N at the ambient pressure, its magnitude is much larger in the intermediate 2-1-coplanar or the IC3 phase with a large quantum spin fluctuation than in the low field phase. We found the pressure induced quantum phases; the *uud* phase for $H \parallel c$ and the IC5 phase for $H \parallel b^*$. We also found the large reduction of the magnetization both below and above T_N and the enhancement of T_N by pressure. dT_N/dP is much larger in the intermediate field phase than in the low field phase. From these results, we could draw the rough magnetic phase diagram under pressure in a high field region. While all the quantum phases below T_N are stabilized by pressure, the degree of the stability by pressure is much larger in the quantum phase with a large quantum spin fluctuation than in the low field phase. In the soft material such as $CsCuCl_3$, we propose that the *ab* plane shrinks spontaneously so as to enhance T_N and the quantum spin fluctuation in high field quantum phases under pressure.

DOI: 10.1103/PhysRevB.96.014419

I. INTRODUCTION

The two-dimensional triangular lattice antiferromagnets (TLAs) have been studied extensively as one of the central issues in the condensed matter physics due to the geometrical frustration [1,2]. When the spins are small, the exotic ground states could be induced by the quantum spin fluctuation. One is the quantum spin liquid ground state. Another is the magnetic order in the TLA with a 120° spin structure [3–8]. The classical ground state of the TLA in magnetic field is infinitely degenerate. There, even very small perturbations can play a crucial role to determine the ground state. The theoretical studies have been performed to elucidate how the degeneracy is lifted by the quantum spin and the thermal fluctuations. The *up-up-down* (*uud*) ground state providing a $M_s/3$ plateau is well known as a typical exotic ground state dominated by such fluctuation effects. Here M_s is the saturation magnetization. Up to now, only few compounds of Cs_2CuBr_4 [9–11] and $Ba_3CoSb_2O_9$ [12–20], etc. are known as the TLA with the *uud* ground state.

$CsCuCl_3$ is well known as the compound in which the appearance of the quantum phase transition was confirmed for the first time [21–23]. $CsCuCl_3$ belongs to the ABX_3 (A = Rb, Cs, B = Mn, Fe, Co, Ni, Cu, and X = Cl, Br) type TLA compounds and has been studied extensively since 1969 by Achiwa [24]. The crystal structure of $CsCuCl_3$ at high temperatures is hexagonal with a space group $P6_3/mmc$ and the $CuCl_6$ octahedra form the chains along the *c* axis by sharing faces. The structural phase transition is induced by the Jahn-Teller effect at 423 K. The crystal structure is changed to that with a space group $P6_122$ or $P6_522$ below 423 K [24–26]. In this low temperature phase, Cu chains along the *c* axis form the helices along the *c* axis with a six periodicity. The Cu spins order antiferromagnetically below $T_N = 10.7$ K [27]. Although the regular triangular lattice with a 120° spin structure in the *ab* plane is maintained below $T_N = 10.7$ K, the helical spin structure along the *c* axis with the incommensurate (IC) wave number $\delta = 0.085$ is realized [27]. Its periodicity is $11.8c-214$ Å. The magnetic properties have been studied extensively [21,22,24,27–32]. The exchange interaction along the *c* axis (J_{ex}^c) is strongly ferromagnetic (FM). It is estimated as large as ∼28 K. These one-dimensional chains form the regular triangular lattice in the *ab* plane and are coupled with the antiferromagnetic (AFM) interaction with $J_{ex}^{ab} \sim -5$ K. The chirality of the Cu chains allows the Dzyaloshinskii-Moriya (DM) interaction with $\boldsymbol{D}$ vector pointing the chain. Its strength is estimated to be $D \sim 5$ K. Below T_N, this compound exhibits a helical magnetic order along the *c* axis with a long period. The nearest neighbor spins along the *c* axis is rotated by $\theta = 5.1°$ [27].

Motokawa *et al.* performed the high field magnetization (M) measurement both for $H \parallel c$ and $H \parallel b^*$ [21,22]. Here b^* is located in the *ab* plane and is perpendicular to the *ac* plane. They discovered the unexpected small discontinuous jump at $H = 12.5$ T for $H \parallel c$ and a plateaulike M-H curve between ∼10 and ∼14 T for $H \parallel b^*$. Nikuni and Shiba showed that the small jump for $H \parallel c$ originates from the quantum phase transition from the umbrella to the 2-1-coplanar phase. There the quantum spin and the thermal fluctuations play an essential role [23]. The umbrella phase is called the IC1 phase [32]. Soon after, the magnetic structure in high magnetic fields for $H \parallel c$ was investigated by Mino *et al.* [33]. In zero magnetic field and the umbrella phase for $H \parallel c$, the $(\frac{1}{3}\frac{1}{3}\delta)$ reflection ($\delta = 0.085$) was observed. In the former, the 120° structure is realized and in the latter, the magnetic moment in the *ab* plane constructs the 120° one. The helical spin structure with the IC wave number δ is realized along the *c* axis. In the umbrella phase, the *c* components of the magnetic moments at all the sublattices are identical. Just above $H_{u\text{-}c} = 12.5$ T, where the

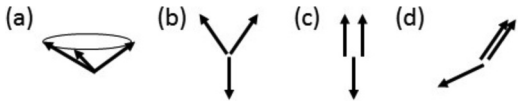

FIG. 1. Four types of spin configurations in the magnetic field: (a) umbrella (b) Y coplanar, (c) *up-up-down* (*uud*), and (d) 2-1-coplanar spin configuration.

umbrella to the 2-1-coplanar phase transition takes place, the intensity of the $(\frac{1}{3}\frac{1}{3}\delta)$ reflection is suddenly suppressed and another reflection of $(\frac{1}{3}\frac{1}{3}0)$ appears. The H dependencies of the intensities of these two reflections exhibits the good agreement with the calculated ones by using the theory by Nikuni and Shiba [23]. Thus, the existence of the 2-1-coplanar structure above $H_{u\text{-}c}$ for $H \parallel c$ was confirmed. The detailed studies of the magnetic structure for $H \parallel b^*$ were also performed by neutron diffraction [34,35]. At $T = 2$ K, the δ value of the $(\frac{1}{3}\frac{1}{3}\delta)$ reflection is reduced with increasing magnetic field. It is very roughly expressed as $\delta = 0.085 - \alpha H^2$ ($\alpha > 0$: constant) in a small magnetic field region. The δ value exhibits a slightly rapid decrease above ∼6 T and a bending at $H \sim$ 10 T and takes a roughly constant value of ∼0.05 between ∼10 and ∼14 T, which is called as the IC3 phase [35]. Above ∼14 T, the δ value decreases rapidly and is zero above ∼16 T, where the commensurate magnetic structure with $(\frac{1}{3}\frac{1}{3}0)$, i.e., the 2-1-coplanar structure, is realized [35]. Although the detailed investigations were performed, the microscopic mechanism of a broad plateau of the M-H curve and roughly constant value of δ between ∼10 and ∼14 T for $H \parallel b^*$ has not yet been clarified [36,37].

In Figs. 1(a)–1(d) we draw the four types of the spin configurations of the TLA in magnetic field, which appears in the present study.

As for the pressure effect on $CsCuCl_3$, which is the main subject in the present paper, it was reported that the δ value increases with increasing pressure [38]. The period of IC magnetic order is reduced by pressure, which leads to the increase of θ between the neighboring spins along the c axis. This means that the DM interaction is enhanced by pressure and the easy-plane magnetic anisotropy originating from the DM interaction is also enhanced.

Recently, this compound attracted attention from the standpoint of the chirality of the crystal structure [39,40].

In $CsCuCl_3$, a large pressure effect on the quantum spin ordered phase is expected from the softness of this compound. This is expected from the small sound velocity [26], small thermal conductivity [41], and the large shrinkage of the lattice constants under pressure [42]. In the present paper, we performed the magnetization measurements of $CsCuCl_3$ both for $H \parallel c$ and $H \parallel b^*$ under pressure and also measured the lattice distortion under the longitudinal magnetic fields at the ambient pressure to clarify how the pressure affects the stability of the quantum phases in magnetic field. We found that the quantum phase transitions are induced in magnetic fields by applying pressure and the intermediate field phases such as the 2-1-coplanar and the *uud* phases are quite stable under pressure.

II. EXPERIMENT

Single crystals of $CsCuCl_3$ were grown from a slightly acidified solution containing CsCl and $CuCl_2 \cdot 2H_2O$ by evaporation of solvent [24]. The magnetization under pressure was measured using the homemade extraction method in magnetic field. The pressure was applied up to ∼0.9 GPa by using a piston cylinder-type pressure cell [43]. The magnetostriction and thermal expansion under the longitudinal magnetic field for $H \parallel b^*$ and $H \parallel c$ were measured by the three terminal capacitance method [44].

III. EXPERIMENTAL RESULTS

A. Magnetization for $H \parallel c$ under pressure

Figures 2(a-1)–2(a-4) show the temperature (T) dependencies of magnetization (M) of $CsCuCl_3$ for $H \parallel c$ under various pressures and Figs. 2(b-1)–2(b-4) their H dependencies. The results at the ambient pressure in Figs. 2(a-1) and 2(b-1) were already reported in our previous paper [19]. Figure 3(a) shows the M-H curves of $CsCuCl_3$ for $H \parallel c$ at $T = 1.5$ K under various pressures. Those in an expanded scale between 10 and 15 T are shown in Fig. 3(b). The characteristic behaviors of M under $P = 0.5$ GPa are similar to those at the ambient pressure. However, its absolute value is significantly reduced both below and above T_N and the magnetization jump (ΔM) at $T_{u\text{-}c}$ is larger than that at the ambient pressure. Here $T_{u\text{-}c}$ is the transition temperature from the umbrella to the 2-1-coplanar phase. Also in the M-H curve, a large jump ΔM is clearly observed at $H_{u\text{-}c}$. Under $P = 0.68$ GPa, while a peak of M at T_N is observed in magnetic field up to 7 T, M shows a significant increase with decreasing temperature below T_N without showing a peak at T_N. ΔM at $T_{u\text{-}c}$ is also larger than that for $P < 0.5$ GPa. Here we should note that in the M-H curve, a plateau of M with ∼0.34 μ_B/Cu appears in a narrow field region between $H_{u\text{-}c}$ and 13.7 T at $T = 1.5$ K under $P = 0.68$ GPa. The magnitude of M is close to $M_s/3$. Namely, this narrow region is strongly suggested to correspond the *uud* phase. The $M_s/3$ plateau observed at $T = 1.5$ K is rapidly smeared out with increasing temperature, although its remnant seems to be recognized up to ∼7 T. Under $P = 0.81$ GPa, a peak of M at T_N is not observed up to 13 T and the magnitude of ΔM is quite large. In the M-H curve at $T = 1.5$ K, after showing a large jump ΔM at $H_{u\text{-}c} = 13.2$ T, there exists a quite narrow field region between 13.2 and 13.7 T where the H-linear increase is observed. Above 13.7 T, the M-H curve exhibits a small slope. This narrow field region might be the new phase and the Y-coplanar phase could be the candidate. Here we note the following characteristic T dependence of M below T_N under $P = 0.81$ GPa above 13.4 T. Above T_N, a separation of each M-T curve is proportional to H, reflecting the H-linear M-H curve in the paramagnetic region as expected. On the other hand, below T_N, this separation becomes smaller with decreasing temperature and it is clearly seen that the M-H curves above $H = 13.4$ T are very much dense below ∼5 T and M at the lowest temperature converges into $\sim M_s/3$.

Figure 4(a) shows the magnetic phase diagrams of $CsCuCl_3$ for $H \parallel c$ under various pressures, where only T_N and $H_{u\text{-}c}$ are drawn. T_N increases with increasing pressure in both umbrella

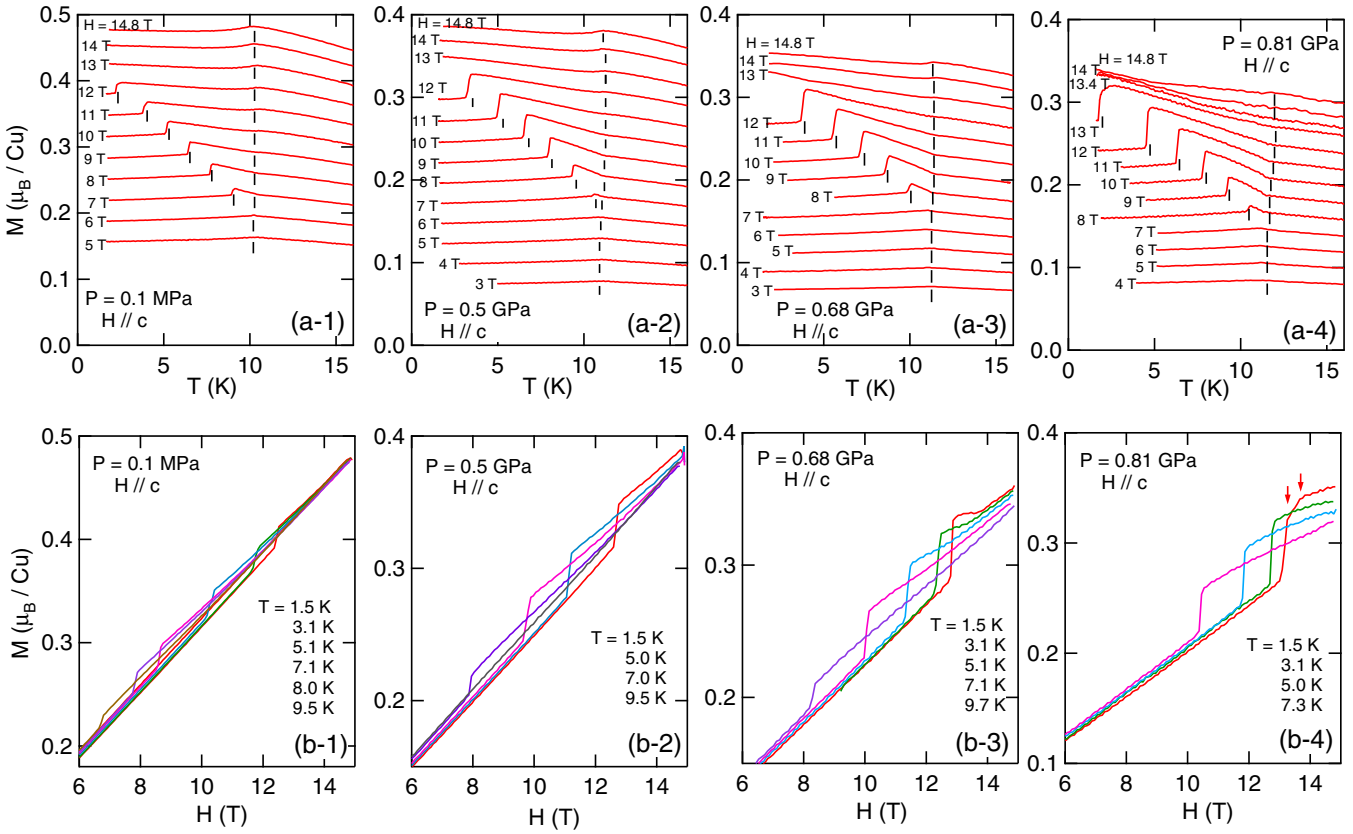

FIG. 2. (a-1)–(a-4) Temperature dependence of the magnetization of $CsCuCl_3$ for $H \parallel c$ measured under $P = 0.1$ MPa, 0.5 GPa, 0.68 GPa, and 0.81 GPa, respectively. (b-1)–(b-4) Magnetization curves of $CsCuCl_3$ for $H \parallel c$ measured under $P = 0.1$ MPa, 0.5 GPa, 0.68 GPa, and 0.81 GPa, respectively. (a-1) and (b-1) are cited from our previous paper [19].

and 2-1-coplanar phases. However, the increasing rate of T_N by pressure (dT_N/dP) is different between these two phases. That in the 2-1-coplanar phase is much larger than that in the umbrella one. Figure 4(b) shows the magnetic phase diagram under $P = 0.68$ GPa. The magnetic field, where the slope of M/H changes at ∼13 T, is plotted by the open triangles and dashed line. Although the region between $H_{u\text{-}c}$ and ∼13 T could be the *uud* phase, its boundary is rapidly smeared out with increasing temperature.

B. Magnetization for $H \parallel b^*$ under pressure

Figure 5(a) shows the T dependence of M of $CsCuCl_3$ for $H \parallel b^*$ under the extremely small pressure and those by the expanded scale around T_N are shown in Fig. 5(b). Here the sample was soaked in Daphne 7373 oil inside the Tefhon cell and was cooled down to 1.5 K and then the magnetization measurements were performed. Here, although the Daphene oil is frozen by cooling down, the extremely small pressure should be applied to the sample. Hereafter, we call this extremely small pressure as $P = 0.1$ MPa (oil). The M-H

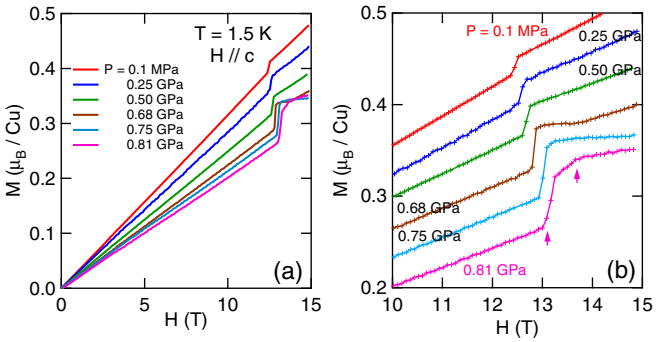

FIG. 3. (a) Magnetization curves of $CsCuCl_3$ for $H \parallel c$ measured at $T = 1.5$ K under various pressures. (b) Those by the expanded scale between 10 and 15 T. The origin of the vertical axis is shifted in each M-H curve.

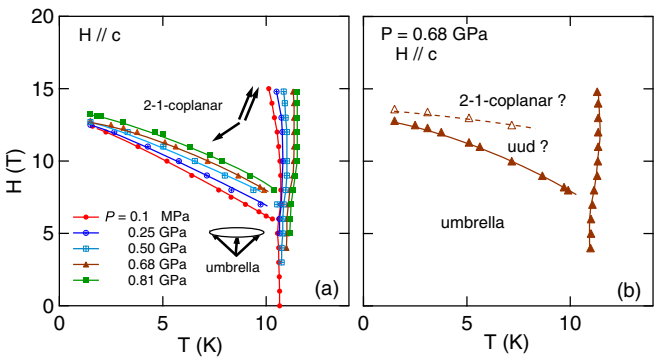

FIG. 4. (a) Magnetic phase diagrams of $CsCuCl_3$ for $H \parallel c$ under various pressures. (b) The magnetic phase diagram for $H \parallel c$ under $P = 0.68$ GPa. See the text for details.

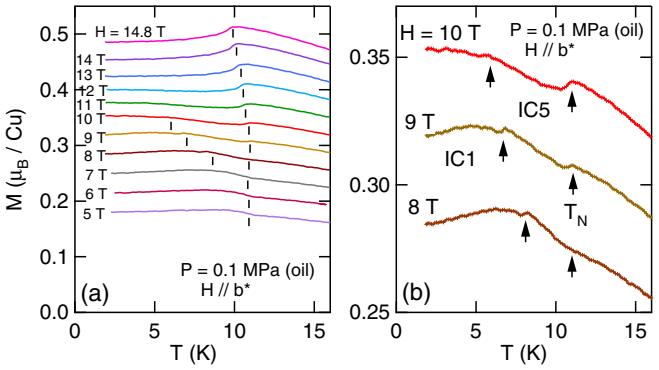

FIG. 5. (a) Temperature dependence of the magnetization of $CsCuCl_3$ for $H \parallel b^*$ under the extremely small pressure obtained by cooling down soaked in oil. See the text for details. (b) Those by the expanded scale between $H = 8$ and 10 T.

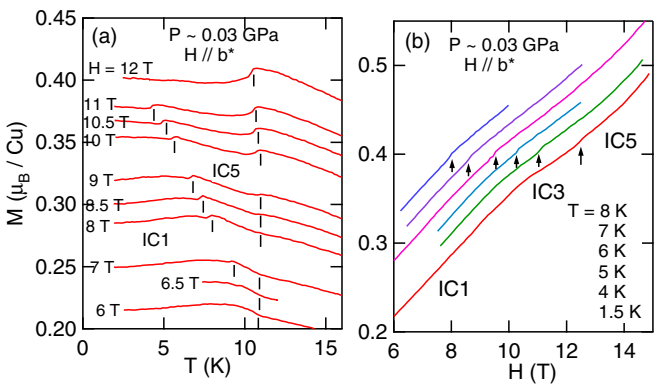

FIG. 6. (a) Temperature dependence of the magnetization for $H \parallel b^*$ of $CsCuCl_3$ under ~0.03 GPa. (b) Magnetization curves of $CsCuCl_3$ for $H \parallel b^*$ under $P \sim 0.03$ GPa. The origin of the vertical axis is shifted in each curve.

curves show almost the same behavior as those at the ambient pressure. However, a small but clear anomaly is recognized between 8 and 10 T in the M-T curves as is shown in Fig. 5(b). These indicate that the IC3 phase is extremely unstable against pressure and the new phase appears in a magnetic field above ~7 T below T_N. As will be discussed later, this new phase is considered as the IC magnetic ordered one. Hereafter, we call this new phase as the IC5 phase. The IC3-IC5 phase transition temperature and transition magnetic field coincide with those of the IC1-IC3 crossover at the ambient pressure above $T \sim 7$ K. However, below ~7 T, the IC1-IC3 crossover field and the transition field (H_{IC5}) are separated. The IC3-IC5 transition accompanied by a small but discontinuous jump ΔM is the first order phase transition. These indicate that once the pressure is applied, even if it is extremely small, the quantum spin fluctuation in the IC5 phase overcomes the DM interaction.

At present, although we do not know if the IC5 phase is commensurate or incommensurate, we conjecture that the IC5 phase is incommensurate, as follows. In the present case, the spins are always located in the ab plane. If the commensurate magnetic order is realized in the IC5 phase, it might be such spin structures as the 2-1-coplanar or the *uud* one. Then it is expected that M shows the roughly H-linear increase in the former and should be constant in the *uud* phase. However, M does not show such H dependencies. Thus, we conclude that the IC magnetic order is realized in the IC5 phase.

Figures 6(a) and 6(b) show the T and H dependencies of M under $P \sim 0.03$ GPa, respectively. $P \sim 0.03$ GPa is also very small pressure. However, ΔM in the M-T curve is much more clearly observed than in Figs. 5(a) and 5(b) in a wide range of magnetic field and temperature. The M-H curve also shows a small ΔM as indicated by the arrows. While the IC1-IC3 crossover exists in the M-H curve at $H \sim 10$ T at $T = 1.5$ K as is observed at the ambient pressure, M shows a small but clear ΔM at $H = 12.5$ T which is the middle of the broad plateau region. With increasing temperature, a shoulder of M accompanied with the IC1-IC3 crossover shifts towards the low magnetic field and at $T = 6$ K, a shoulder disappears and the direct IC1-IC5 phase transition takes place.

Figures 7(a-1)–7(a-4) represent the T dependencies of M for $H \parallel b^*$ under various pressures and Figs. 7(b-1)–7(b-4) their H dependencies. Figure 8 shows the M-H curves for $H \parallel b^*$ at $T = 1.5$ K under various pressures. The magnitude of M decreases significantly with increasing pressure both below and above T_N in the same as for $H \parallel c$. In magnetic fields below ~6 T, M exhibits a broad shoulder slightly below T_N in the M-T curve. ΔM is observed at the IC3-IC5 or the IC1-IC5 phase transition. The magnitude of ΔM increases with increasing pressure. However, it is still much smaller than that for $H \parallel c$. The T dependence of M for $H > 7$ T below T_N is different between the low and high pressure regions. Although M shows almost a T-linear increase with decreasing temperature below T_N under low pressures, it shows a convex T dependence below T_N for $P > 0.61$ GPa. This is clearly seen when the M-H curves at $H = 9$ T under $P = 0.21$ and 0.94 GPa are compared. In the high field region between 12 and 15 T, M increases with decreasing temperature below T_N without showing a peak at T_N under high pressures, while M exhibits a peak at T_N under low pressures. The magnetic field of a shoulder of the M-H curve shifts towards the higher magnetic field with increasing pressure. While a broad shoulder is seen at ~11.5T under $P = 0.35$ GPa, for $P > 0.61$ GPa, M exhibits an H-linear increase up to H_{IC5} without showing a shoulder. ΔM at this transition field is much larger than that under $P = 0.35$ GPa. The slope of M/H in the IC5 phase is smaller than that in the IC1 phase.

Figure 9 shows the magnetic phase diagrams of $CsCuCl_3$ for $H \parallel b^*$ under pressure. The IC1-IC3 transition at the ambient pressure is a broad crossover, which is drawn by a dotted red line. However, by applying the extremely small pressure, the first order IC3-IC5 phase transition appears in the middle of the plateau region. Although T_N is enhanced by pressure, the magnitude of dT_N/dP is different between the low field and the intermediate field phases. dT_N/dP in the IC5 phase is much larger than that in the IC1 phase. Under $P = 0.94$ GPa, T_N at $H = 14.8$ T increases from 9.8 to 12 K. The increase of T_N is as large as 2.2 K. It is known that the first order IC3-C phase transition takes place at ~16 T at the ambient pressure as is indicated by the red solid line [35,40]. We expect that the IC5-C phase transition exits also under pressure and its transition field increases with increasing pressure. The crossover boundary between the IC4 and IC1 phases at the ambient pressure is shown by a dashed line

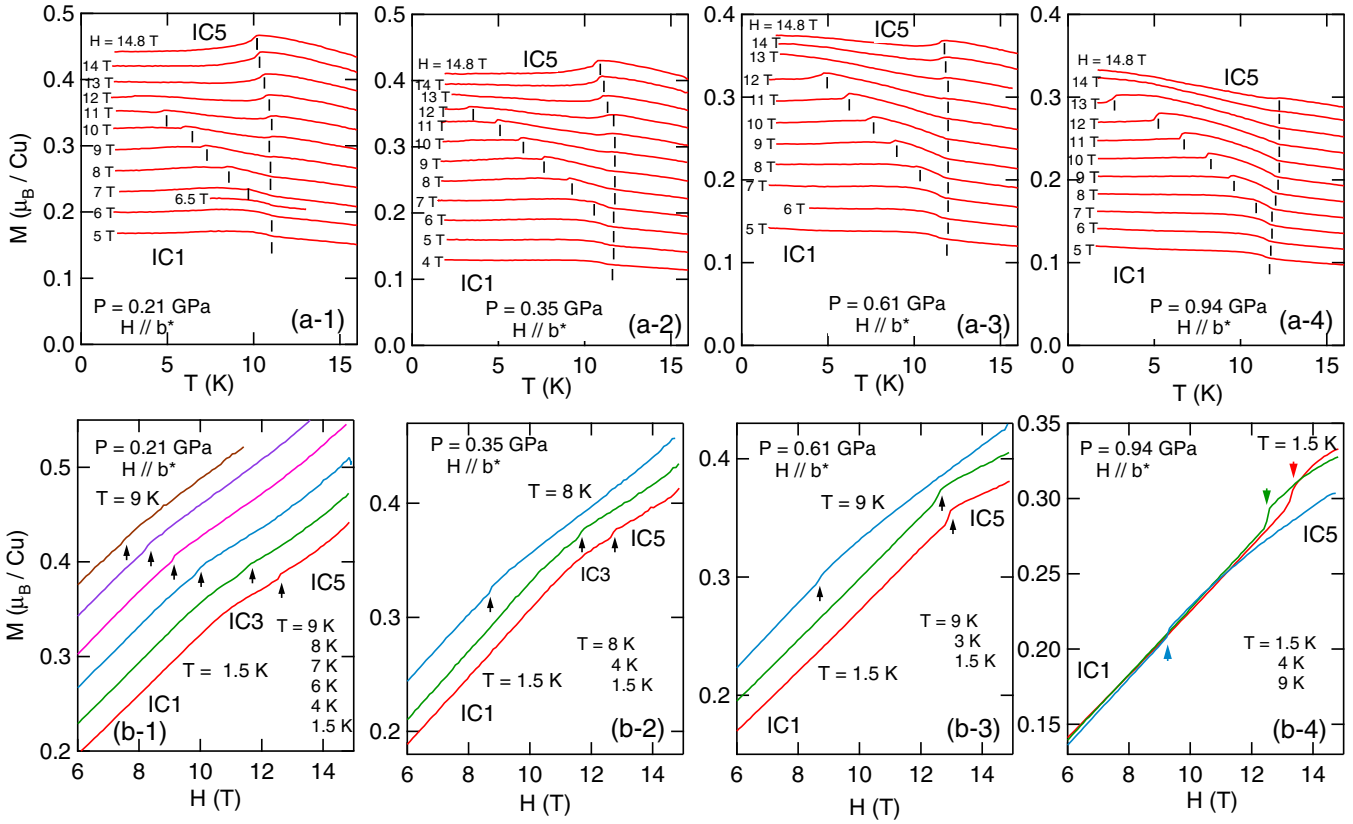

FIG. 7. (a-1)–(a-4) Temperature dependence of the magnetization of $CsCuCl_3$ for $H \parallel b^*$ measured under $P = 0.21$, 0.35, 0.61, and 0.94 GPa, respectively. (b-1)–(b-4) Magnetization curves of $CsCuCl_3$ for $H \parallel b^*$ measured under $P = 0.21$, 0.35, 0.61, and 0.94 GPa, respectively. The vertical axis of the magnetization is shifted in each curve in (b-1)–(b-3).

in Fig. 9, which is estimated from a shoulder of the M-T curve. This crossover boundary disappears rapidly by applying pressure and it is replaced by the first order phase transition between the IC1 and IC5 phases.

C. Pressure dependence of T_N

In the present experiments, T_N is found to be enhanced by pressure. The magnitude of dT_N/dP is different between the low field and the intermediate field phases. Figure 10 shows the pressure dependence of T_N for $H \parallel b^*$ and $H \parallel c$, both in the low field ($H = 5$ T) and intermediate field ($H = 14.8$ T) phases. In the IC1 phase, dT_N/dP is small. It is ~0.83 K/GPa

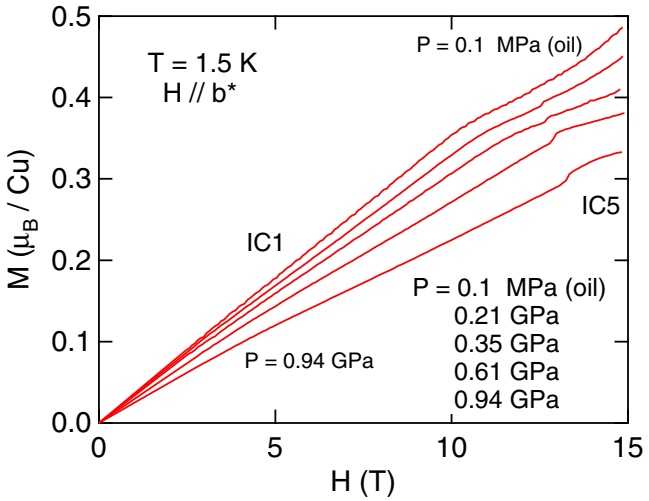

FIG. 8. Magnetization curves of $CsCuCl_3$ for $H \parallel b^*$ at $T = 1.5$ K under various pressures. See the text for details.

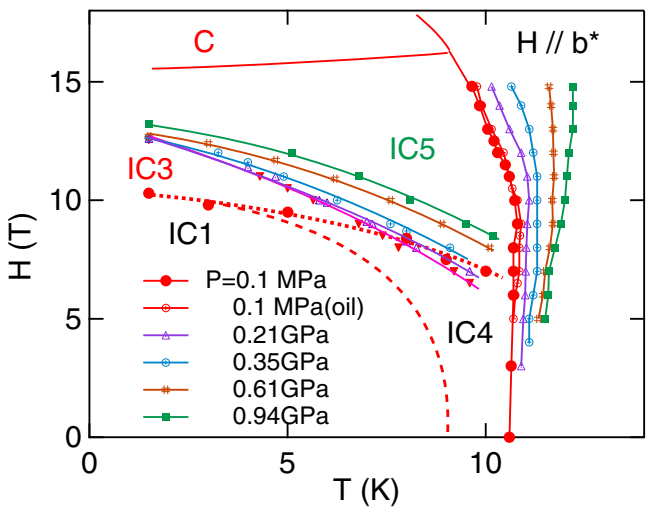

FIG. 9. The magnetic phase diagrams of $CsCuCl_3$ for $H \parallel b^*$ under various pressures. The IC1-IC3 crossover boundary at the ambient pressure is cited from Ref. [19] and the IC3-C phase boundary is cited from Refs. [35,40]. The crossover boundary between the IC1 and IC4 phases at the ambient pressure is drawn by a dashed line. See the text for details.

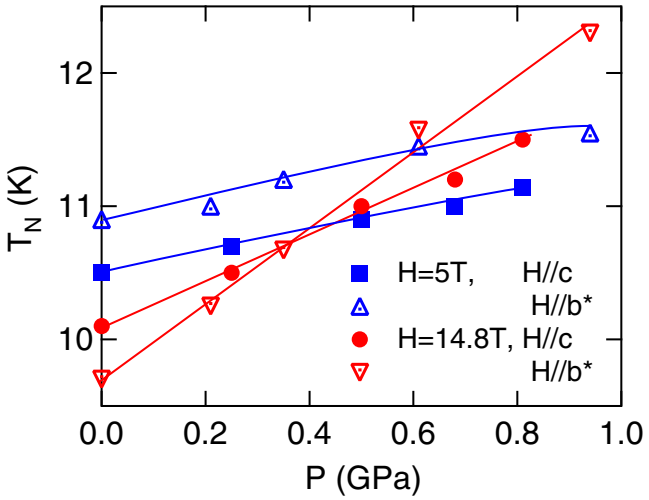

FIG. 10. Pressure dependence of T_N of $CsCuCl_3$ for $H \parallel c$ and b^* at $H = 5$ and 14.8 T, respectively.

and is almost isotropic. On the other hand, that in the 2-1-coplanar or the IC5 phase is much larger than that in the IC1 phase. Furthermore, it exhibits a large anisotropy. That in the IC5 phase for $H \parallel b^*$ is $\sim$2.77 K/GPa at $H = 14.8$ T and that in the 2-1-coplanar phase for $H \parallel c$ is $\sim$1.73 K/GPa. dT_N/dP at $H = 14.8$ T is larger for $H \parallel b^*$ than for $H \parallel c$. This indicates that dT_N/dP is larger when the spins are located in the ab plane, which is favorable for the easy-plane magnetic anisotropy. The important information on the stability of the quantum phase in magnetic fields could be obtained from the pressure dependence of T_N.

D. Lattice distortion under the longitudinal magnetic field at the ambient pressure

The important information on the stability of the quantum phases could be obtained by combining the anisotropic lattice distortion at the ambient pressure and dT_N/dP in magnetic fields. Here we present the lattice distortion in magnetic fields.

Figures 11(a) and 11(b) show the magnetostriction and the thermal expansion of $CsCuCl_3$ under the longitudinal magnetic field $H \parallel c$ at the ambient pressure, respectively. In the paramagnetic region, the c axis expands proportional to H^2 as usual. The similar H^2-like behavior is also observed in the umbrella phase, although the magnitude of the variation is much larger than in the paramagnetic region. At $H_{u\text{-}c}$, a discontinuous jump is observed and slightly above $H_{u\text{-}c}$, the variation is small. In zero magnetic field, the c axis shows a small expansion below T_N assuming the lattice thermal expansion as shown by the dashed line in Fig. 11(b). Although the expansion due to the magnetic origin below T_N increases with increasing magnetic field, it is small at low magnetic fields in the umbrella phase. In the 2-1-coplanar phase, the c axis expands significantly with decreasing temperature below T_N. Above $\sim$7 T, the transition from the coplanar to the umbrella phase exists at $T_{u\text{-}c}$, where a large discontinuous change is observed.

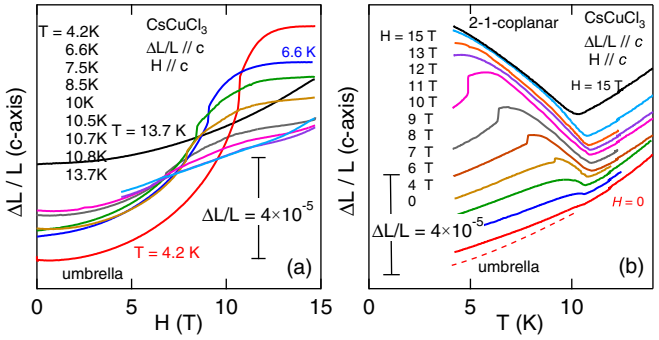

FIG. 11. (a) Longitudinal magnetostriction of $CsCuCl_3$ for $H \parallel c$ at the ambient pressure. (b) Thermal expansion of $CsCuCl_3$ under the longitudinal magnetic field $H \parallel c$ at the ambient pressure. The dashed line at $H = 0$ indicates the lattice thermal expansion roughly estimated from the high temperature region.

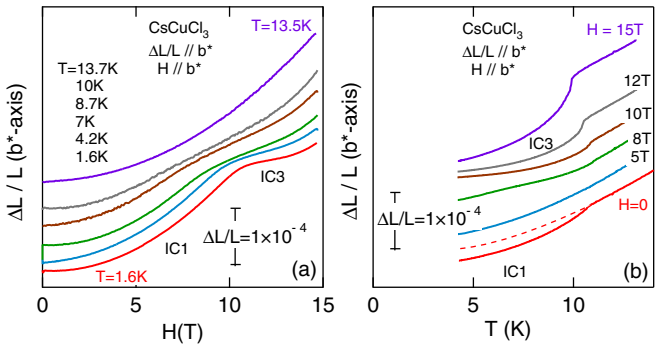

FIG. 12. (a) Longitudinal magnetostriction of $CsCuCl_3$ for $H \parallel b^*$ at the ambient pressure. (b) Thermal expansion of $CsCuCl_3$ under the longitudinal magnetic field $H \parallel b^*$ at the ambient pressure. The dashed line at $H = 0$ indicates the lattice thermal expansion roughly estimated from the high temperature region.

Figures 12(a) and 12(b) show the magnetostriction and the thermal expansion of $CsCuCl_3$ under the longitudinal magnetic field $H \parallel b^*$ at the ambient pressure, respectively. In the paramagnetic region, the b^* axis exhibits the H^2-like behavior as in the case of $H \parallel c$. The similar H dependence is observed also in the IC1 phase, while the magnitude of the variation is larger than in the paramagnetic region. The b^* axis exhibits a broad shoulder at the IC1-IC3 crossover field of $\sim$10 T and is nearly constant in the IC3 phase between $\sim$11 and $\sim$14 T at $T = 1.5$ K. The shoulder at the IC1-IC3 crossover field is rapidly smeared out with increasing temperature. In zero magnetic field, the b^* axis shows a small shrinkage below T_N assuming the lattice thermal expansion as shown by the dashed line in Fig. 12(b). At $H = 5$ T, no anomaly is observed at T_N. This is because $H = 5$ T is close to the IC1-IC3 crossover field showing a shoulder in the magnetostriction at T_N. With further increase of H, a shrinkage below T_N becomes pronounced.

IV. DISCUSSION

A. Magnetic phase diagram under pressure

The magnetization of $CsCuCl_3$ was not measured in a high field region in the present experiments. However, it is possible to conjecture the M-H curves and the magnetic phase diagrams in a higher magnetic field region by using the

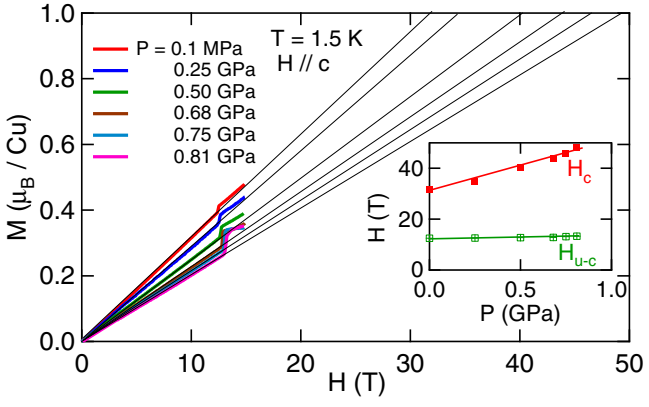

FIG. 13. Magnetization curves of $CsCuCl_3$ for $H \parallel c$ at $T = 1.5$ K under various pressures. The straight black line indicates the M-H curve up to H_c obtained by assuming the same slope of M/H in the umbrella phase. The inset shows the pressure dependence of H_c indicated by a red line and $H_{u\text{-}c}$ indicated by a green line. We note that the slope of M/H in the 2-1-coplanar phase is not correct but should be smaller than that in the figure. See the text for details.

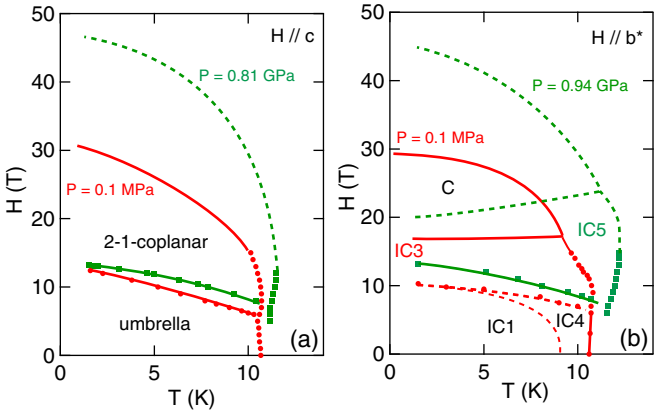

FIG. 14. (a) Magnetic phase diagram for $H \parallel c$ at the ambient pressure (red solid line) and conjectured magnetic phase diagram for $P = 0.81$ GPa (green dotted line). The *uud* phase under $P = 0.81$ GPa is not shown. (b) Magnetic phase diagram for $H \parallel b^*$ at the ambient pressure (red solid line) and conjectured magnetic phase diagram for $P = 0.94$ GPa (green dotted line). The magnetic phase diagrams above 15 T at the ambient pressure are cited from Refs. [21,22,40] and those below 15 T are from Ref. [19]. In the estimation H_c under pressure, there exists an ambiguity. See the text for details.

present results. Here we should note that the saturation field (H_c) should be enhanced significantly by pressure, considering that M is significantly reduced both below and above T_N by pressure. Below, we consider the expected magnetic phase diagrams under pressure both for $H \parallel c$ and $H \parallel b^*$.

First, we consider the magnetic phase diagram for $H \parallel c$ under pressure. The black solid straight lines in Fig. 13 are the expected M-H curves in a high field region at $T = 1.5$ K under various pressures. Each of these lines shows the M-H curve with the slope of M/H in the umbrella phase. Here we assume that the slope of M/H in the 2-1-coplanar phase is the same as that in the umbrella phase. Then we can make a rough estimation of H_c as the magnetic field where M reaches to M_s. Here M_s is assumed to be 1 μ_B/Cu, for simplicity. We note that as for the estimated value of H_c for $P > 0.68$ GPa, there exits a larger ambiguity than that for $P < 0.5$ GPa because there exits a plateau M-H region in the intermediate magnetic fields for $P > 0.68$ GPa. We also note that the slope of M/H in the high field 2-1-coplanar phase under pressure should be smaller than that in the umbrella phase due to the larger increasing rate of dT_N/dP. However, since it is difficult to estimate its slope in the high field phase, here we draw the straight line with the same slope as that in the umbrella phase. Thereby, there exists also the ambiguity in the estimation of H_c. The estimated value of $H_c \sim 30$ T at the ambient pressure is consistent with the experimental results [21,22,40]. With increasing pressure, the slope of M/H is suppressed and H_c increases. H_c under $P = 0.81$ GPa is estimated to be ~48 T. The obtained pressure dependence of H_c and the experimental results of $H_{u\text{-}c}$ are shown in the inset of Fig. 13. The estimated H_c exhibits the significant increase with increasing pressure. On the other hand, the increase of $H_{u\text{-}c}$ is much smaller than that of H_c.

Figure 14(a) shows the conjectured magnetic phase diagram for $H \parallel c$ under $P = 0.81$ GPa together with that at the ambient pressure. The *uud* phase under $P = 0.81$ GPa is not shown. The magnetic phase diagram in a high field region is shown by a green dashed line, which is conjectured by using the above estimated H_c and the H dependence of T_N up to $H = 14.8$ T. This indicates that both low field umbrella and intermediate field 2-1-coplanar phase are stabilized by pressure. However, the pressure effect is very different between these two phases. Although the increasing rates of T_N and $H_{u\text{-}c}$ by pressure in the umbrella phase is small, T_N and H_c in the 2-1-coplanar or the *uud* phase are quite large.

Next, we consider the magnetic phase diagram for $H \parallel b^*$ under pressure. In a low pressure region, it is difficult to estimate H_c by using the slope of M/H in a low field region because of the existence of the shoulder in the M-H curve at $H \sim 10$ T. On the other hand, for $P > 0.61$ GPa, M shows a roughly H-linear increase up to H_{IC5}. Then, it is possible to make a rough estimation of H_c. H_c for $P = 0.94$ GPa is estimated to be ~45 T. This value is not so different from ~48 T for $H \parallel c$ at $P = 0.81$ GPa. The conjectured magnetic phase diagram for $H \parallel b^*$ under $P = 0.94$ GPa is shown by the green dashed lines in Fig. 14(b). This magnetic phase diagram might be plausible as a rough estimation, although there exists a large ambiguity in the estimation of H_{IC5}. As in the case for $H \parallel c$, dT_N/dP in the IC1 phase is small. However, those in the IC5 and the C phases are large. Namely, the intermediate and the high field phases are significantly expanded by pressure compared with the small expansion in the IC1 phase region.

The different stability between the low field and the intermediate or the high field phases under pressure should originate from the different magnitude of dT_N/dP between these two phases. The important information on the exchange interaction could be obtained from the magnetization in the paramagnetic region. The magnitude of M is significantly reduced by pressure both below and above T_N and T_N is enhanced by pressure. dT_N/dP might be proportional to dJ_{ex}^{ab}/dP. J_{ex}^{ab} is the in-plane AFM interaction. Then, H_c is

also expected to shift towards higher field. This is consistent with the expectation that H_c increases significantly by pressure as a result of the large reduction of M both below and above T_N, as mentioned before. Although the interplane FM exchange interaction along the c axis (J_{ex}^c) also should be affected by pressure, it is difficult to discuss the pressure dependence of J_{ex}^c in the present experiments. On the other hand, the theoretical studies showed that H_c is not affected by J_{ex}^c when the exchange interaction along the c axis is that of the Heisenberg type [45,46]. Thereby, hereafter, we do not consider the pressure effect of J_{ex}^c.

Here we emphasize the softness of $CsCuCl_3$. The softness of the crystal induces the large pressure effect on the magnetic properties. The large and anisotropic lattice shrinkages of $CsCuCl_3$ by pressure at room temperature were reported by Christy *et al.* [42]. The shrinkage of the lattice constants by pressure is as large as ∼1%/GPa. This indicates that $CsCuCl_3$ is a very soft material. This is supported by the small sound velocity (v_s) and the small thermal conductivity ($\kappa \sim \kappa_{ph} = \frac{1}{3} C_{ph} v_s l$) at high temperatures. Here C_{ph} and l are the phonon specific heat and the phonon mean free path. In $CsCuCl_3$, v_s for the C_{44} mode at 300 K is as small as ∼1200 m/s [26] and κ at 100 K is ∼1.2 W/K m [41]. These values are much smaller than $v_s = 5100$ m/s for the longitudinal sound wave and 2800 m/s for the transverse one [18] and $\kappa \sim 8$ W/K m [15], in the typical TLA compound of $Ba_3CoSb_2O_9$. Then, we expect the large pressure effect on the exchange interaction in $CsCuCl_3$. Furthermore, the large anisotropic shrinkage of the lattice constant was observed in this compound. The shrinkage of the a axis is 30% larger than that of the c axis [42]. This anisotropic lattice distortion is expected to be enhanced by pressure below T_N. Considering that T_N is enhanced by pressure, the shrinkage of the ab plane enhanced by pressure plays an important role in the stabilization of the quantum phases in magnetic fields. In zero magnetic field at the ambient pressure, already the anisotropic lattice distortion is observed below T_N. There exists a small expansion of the c axis and a small shrinkage of the b^* axis below T_N as is seen in Figs. 11(b) and 12(b), respectively.

As for the lattice distortion in magnetic fields at the ambient pressure, since the measurements were performed only under the longitudinal magnetic field, it is difficult to clarify the anisotropic lattice distortion, exactly. However, it is possible to derive its information by combining the results of the thermal expansion at the ambient pressure and the magnitude of dT_N/dP in magnetic fields. The experiments clearly show that the magnitude of the lattice distortion is much larger in the intermediate field phase than in the low magnetic field phase. For $H \parallel c$, the ab plane should shrink significantly below T_N by pressure to be consistent with the large enhancement of T_N by pressure and the significant expansion of the c axis in the 2-1-coplanar phase below T_N. For $H \parallel b^*$, the b^* axis in the IC3 phase shrinks significantly below T_N. Thus, the shrinkage of the ab plane is much larger in the intermediate field phase than in the IC1 phase. This large shrinkage of the ab plane should be the origin of the large enhancement of T_N and H_c in the intermediate or the high field phase by pressure.

Before discussing the magnetic properties both for $H \parallel c$ and $H \parallel b^*$ under pressure, we note the following three characteristics. (i) The largest energy gain of the quantum spin and the thermal fluctuations is obtained in the (1D) collinear, the second the (2D) coplanar, and the third the (3D) umbrella spin structure. (ii) the maximum energy gain of the quantum spin fluctuation is obtained when the *uud* collinear spin structure with $M_s/3$ is realized. Then we expect that when the magnetic field increases and M is closed to $M_s/3$, the spin structure has a tendency to construct a plateaulike M-H curve with $M \sim M_s/3$ to obtain the largest energy gain of the quantum spin fluctuation. This characteristics might be the origin of the plateaulike M-H curve in the IC3 phase for $H \parallel b^*$, although the IC magnetic ordering is realized in this phase. (iii) the stronger the quantum spin fluctuation, the higher the Néel temperature T_N.

B. Pressure effect for $H \parallel c$

First, we discuss the reason why the *uud* phase is induced for $H \parallel c$ by pressure. Generally, the competition between the quantum spin fluctuation and the magnetic anisotropy of the anisotropic exchange interaction determines which type of the quantum phase is stable in magnetic fields. Of course, this should be too simplified to apply the calculated result to the 3D real compound. In $CsCuCl_3$, there exist the strong ferromagnetic interaction along the c axis, DM interaction, and single ion magnetic anisotropy except the in-plane exchange one (J_{ex}^{ab}). It is reported that the DM interaction is enhanced by pressure [38]. This induces the enhancement of the easy-plane magnetic anisotropy and suppresses the quantum spin fluctuation and makes the appearance of the Y-coplanar or the *uud* phase difficult. This discrepancy might be explained by considering the larger increasing rate of dT_N/dP in the high field quantum phases than in the low field umbrella phase. At the ambient pressure, the magnetic anisotropy overcomes the quantum spin fluctuation and the transition from the umbrella to the 2-1-coplanar phase takes place. Both magnetic anisotropy and J_{ex}^{ab} are enhanced by pressure. The present result that the quantum phases such as Y-coplanar or *uud* phase appears under pressure indicates that the enhancement of the magnetic anisotropy by pressure is smaller than that of J_{ex}^{ab} in the high field quantum phases. Here we note the relation between the different types of the lattice distortion and the different increasing rate of dT_N/dP between the low field and high field quantum phases. The origin of the enhancement of the spin fluctuation is the increase of T_N by pressure. Namely, the higher T_N, the larger the quantum spin fluctuation. In the umbrella phase with a small increasing rate of dT_N/dP, the quantum spin fluctuation is small. However, in the high field phase with a large magnitude of dT_N/dP, the spin quantum fluctuation is large and the Y-coplanar or the *uud* phase appears. The reason why the magnitude of dT_N/dP is larger in the high field phases than in the low field umbrella phase is the anisotropic lattice distortion, i.e., a large shrinkage of the crystal takes place spontaneously so as to enhance T_N and the spin fluctuation. In other words, a large shrinkage of the ab plane assists the enhancement of T_N and spin fluctuation in the high field quantum phase.

The information on the competition between the easy-plane magnetic anisotropy and the quantum spin fluctuation could be observed in Fig. 15. The red squares and blue circles in Fig. 15 represent the magnitude of M at $H = 12.5$ and 13

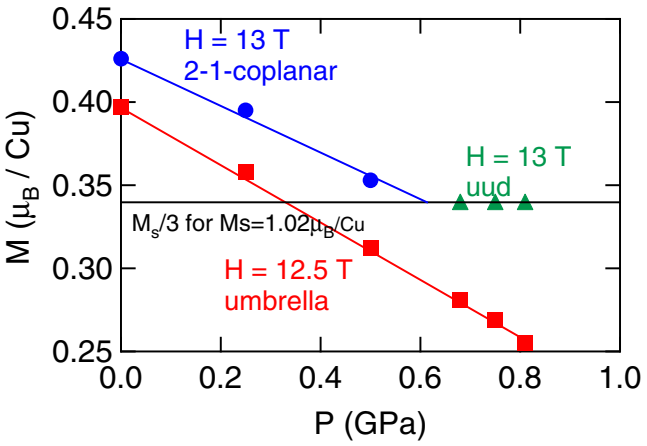

FIG. 15. Pressure dependence of the magnetization at $H = 12.5$ and 13 T at $T = 1.5$ K, respectively.

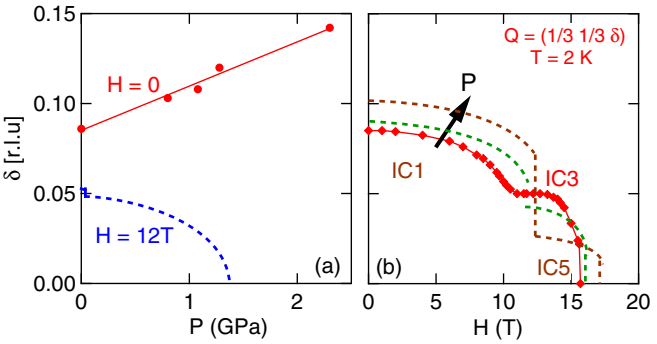

FIG. 16. (a) Pressure dependence of the IC wave number δ at $H = 0$ and 12 T. That at $H = 0$ is cited from Ref. [38]. The blue dashed line indicates the speculated H dependence of δ at $H = 12$ T. (b) Speculated magnetic field dependence of δ at $T = 2$ K under pressure. The brown and green dashed lines indicate the expected H dependence of δ for high and intermediate pressure, respectively.

T under pressure at $T = 1.5$ K, respectively. The magnitude of M at $H = 13$ T for $P > 0.6$ GPa is shown by the green triangle. These two magnetic fields correspond to those just below and above $H_{u\text{-}c}$. The former belongs to the umbrella phase and the latter to the 2-1-coplanar one. Here we note that for $P = 0.81$ GPa, we plotted the extrapolated value to $H = 13$ T from the high field M-H curve. The horizontal black line corresponds to $M_s/3$ assuming that $M_s = 1.02\ \mu_B$/Cu.

At the ambient pressure, the magnitude of M for $H \parallel c$ at $H = 12.5$ T is $\sim 0.4\ \mu_B$/Cu. This value is larger than $M_s/3$. Namely, the umbrella phase is stable even though M is larger than $M_s/3$. This should be due to the large energy gain of the easy-plane magnetic anisotropy, which overcomes that of the quantum spin fluctuation. When the pressure is applied, although the easy-plane magnetic anisotropy is enhanced, at the same time, M is significantly reduced both below and above T_N. M at $H = 12.5$ T continues to decrease with increasing pressure. On the other hand, M at $H = 13$ T decreases up to $P = 0.6$ GPa and takes the roughly constant value of $\sim 0.34\ \mu_B$/Cu $\sim M_s/3$ above $P \sim 0.6$ GPa. The $M_s/3$ value acts as a stopper in which M could not take a smaller value than $M_s/3$ because the largest energy gain of the quantum spin fluctuation is obtained in the *uud* phase.

Although the *uud* spin structure is strongly suggested to be realized in the $M_s/3$ plateau region, it should be examined by the neutron diffraction experiments in magnetic fields under pressure. In the *uud* phase, there exist the three domains along the c axis. At present, we do not know its domain size and its distribution. Namely, the domain distribution is completely at random or there exists a long range period along the c axis as was observed in the 2-1-coplanar phase for $H \parallel c$ at the ambient pressure [33]. The transition from the *uud* to the 2-1-coplanar phase under pressure also should be examined by the neutron diffraction.

C. Pressure effect for $H \parallel b^*$

First, we discuss the H dependencies of M and δ at the ambient pressure. The spins are located always in the ab plane for $H \parallel b^*$ due to the easy-plane magnetic anisotropy. At the ambient pressure, the M-H curve shows the IC1-IC3 crossover at $H \sim 10$ T. In the IC3 phase between $\sim$10 and $\sim$14 T, M shows a plateaulike behavior. This is because when M is close to $M_s/3$ in the process of the increasing magnetic field, the spin structure has a tendency to construct the *uud* structure with the largest energy gain of the quantum spin fluctuation. However, in $CsCuCl_3$, the *uud* structure cannot be realized due to the existence of the DM interaction. At low magnetic fields in the IC1 phase, δ behaves approximately as $\delta \sim 0.085 - \alpha H^2$. After showing a broad shoulder at $H \sim 10$ T, δ shows a plateaulike behavior in the IC3 phase [35]. Thus, M and δ are strongly coupled with each other. In a low field region, the DM interaction is dominant and the helical spin structure is maintained although it is modified slightly. The $2Q$ harmonics appears above $\sim$6 T and the $4Q$ one in the IC3 phase [35]. In the IC3 phase, although the helical spin structure with $\delta \sim 0.05$ is realized, it should be significantly modified. In the IC3 phase, we expect that the spin structure similar to the *uud* one might appear in the intermediate region within the long range period and the helical spin rotation could be realized around both ends of the long period. Both ends of the long period structure could be viewed as the domain wall. Such a spin structure was discussed by Stusser *et al.* [35]. They discussed the possibility of spin structure in the IC3 phase that consists of a sequence of six suitably different 2-1-domains separated by domain wall as is shown in Fig. 9 in Ref. [35]. Here we note that since M of $\sim 0.4\ \mu_B$/Cu in the IC3 phase is larger than $M_s/3$, the down spin in the 2-1-domain in Fig. 9 in Ref. [35] should be canted significantly from the c axis. With further increase of magnetic field, δ decreases furthermore and the above domain walls could be changed to the isolated soliton proposed by Miyake *et al.* [40].

Now we discuss the pressure effect on the M-H and the $\delta - H$ curves for $H \parallel b^*$. δ in zero magnetic field increases by applying pressure as shown in Fig. 16(a) [38]. This indicates the enhancement of the DM interaction by pressure, which leads to the increase of θ. Then it might be difficult to reduce δ by magnetic field and the suppression of the quantum spin fluctuation is larger than that at the ambient pressure. Then $\delta = \delta_0 - \beta H^2$ ($\beta < \alpha$) behavior is expected in a low field region under pressure. However, the magnetic field where the

slightly rapid decrease of δ is observed shifts towards the higher magnetic field than ∼6 T at the ambient pressure. Here δ_0 is δ in zero magnetic field under pressure. Thus, the magnetic field of the shoulder in the M-H curve shifts towards the higher magnetic field and the magnetic field region where the M shows an H-linear increase expands to the higher magnetic field. When the magnetic field increases, there should exist a magnetic field region where the magnitude of M is close to $M_s/3$. δ_0 under pressure is larger than that at the ambient pressure. With increasing pressure, this magnetic field region meets with that showing $\delta = \delta_0 - \beta H^2$ behavior. Then the IC1-IC3 crossover disappears and in its place, the first order IC1-IC5 transition appears. The experimental results show that the slope of M/H in the IC5 phase is reduced with increasing pressure and the magnitude of M in this region becomes close to $M_s/3$. These suggest that the spin structure similar to the *uud* phase could be realized in the IC5 phase, although the IC magnetic order probably with a small magnitude of δ is realized. Thus, with increasing pressure, although δ_0 is enhanced by pressure, we conjecture that δ above $H = 12$ T is suppressed with increasing pressure. These are drawn in Fig. 16(a). The speculated H dependence of δ under various pressures is shown in Fig. 16(b).

In the pressure effect for $H \parallel b^*$, there remain the following problems to be clarified. (1) Why the IC5 phase appears under so extremely small pressure [$P = 0.1$ MPa (oil)]? The ambient pressure looks like even the critical pressure above which the IC5 phase appears. (2) Why the IC3-IC5 or the IC1-IC5 phase transition is that of the first order? Since the change of δ is expected to be quite small under very small pressure, we simply expect the continuous change of δ at this transition. However, this is not the case. (3) What kind of the interaction triggers the transition to the IC5 phase? Although it should be associated with the applied pressure, the pressure is extremely small. These problems should be clarified in the future.

V. CONCLUSION

We investigated the pressure effect on the magnetization of the soft material $CsCuCl_3$ both for $H \parallel c$ and $H \parallel b^*$. We also measured the lattice distortion under the longitudinal magnetic fields at the ambient pressure. At the ambient pressure, the ab plane shrinks in all the quantum phases below T_N. However, its magnitude is significantly different between the low field IC1 phase and the intermediate 2-1-coplanar or the IC3 phase. It is much larger in the latter phases with a large quantum spin fluctuation than in the former phase. Such a lattice distortion depending on the spin structure should be enhanced by pressure. We found the pressure induced new phases both for $H \parallel c$ and $H \parallel b^*$. The *uud* phase for $H \parallel c$ and the IC5 phase for $H \parallel b^*$. We also found the large reduction of M both below and above T_N under pressure and the enhancement of T_N by pressure which is significantly different between the IC1 phase and the 2-1-coplanar or the IC3 phase. dT_N/dP is small in the IC1 phase but is much larger in the 2-1-coplanar or the IC3 phase. From these results, we could draw the rough magnetic phase diagram under pressure in a high field region. All the quantum phases below T_N are stabilized by pressure. However, the degree of the stability is very different between the IC1 phase and the 2-1-coplanar or the IC3 phase. It is much larger in the latter than in the former. The degree of the stability by pressure is large in the quantum phase where the large energy gain of the quantum spin fluctuation is obtained but is small in the IC1 phase. The relation of "the stronger the quantum spin fluctuation, the higher the Néel temperature T_N" is obtained in the present study. In the soft material such as $CsCuCl_3$, it is possible to distort the crystal structure spontaneously so as to enhance T_N and the quantum spin fluctuation in the high field quantum phases. The pressure induced *uud* phase for $H \parallel c$ could be explained by the competition between the easy-plane magnetic anisotropy enhanced by pressure and the spontaneous shrinkage of the ab plane assists the enhancement of T_N and the quantum spin fluctuation. We found the pressure induced new IC5 phase by the extremely small pressure for $H \parallel b^*$. Why the IC5 phase appears under so extremely small pressure should be clarified in the future.

ACKNOWLEDGMENTS

The authors would like to thank H. Ohta, T. Sakurai, S. Okubo, T. Kawamata, Y. Koike, H. Shiba, S. Yamamoto, and Y. Kamiya for stimulating discussions. The authors acknowledge the support from the JSPS Grant-Aid Scientific Research (S) (No. 25220803) "Towards a New Class Magnetism by Chemistry-controlled Chirarity," the JSPS Grant-Aid for Scientific Research (C) (No. 26400368), the JSPS Grant-Aid for Scientific Research on Innovative Areas (No. 15H05885), and the Center for Chiral Science in Hiroshima University (the MEXT program for promoting the enhancement of research universities, Japan).

[1] P. W. Anderson, Mater. Res. Bull. **8**, 153 (1973).
[2] L. Balents, Nature (London) **464**, 199 (2010).
[3] H. Kawamura, Proc. Phys. Soc. Jpn. **53**, 2452 (1984).
[4] H. Kawamura and S. Miyashita, J. Phys. Soc. Jpn. **54**, 4530 (1985).
[5] A. V. Chubukov and D. I. Golosov, J. Phys. C: Solid State Phys. **3**, 69 (1991).
[6] S. Watarai, S. Miyashita, and H. Shiba, J. Phys. Soc. Jpn. **70**, 532 (2001).
[7] S. Miyashita, Proc. Jpn. Acad. Ser. B **86**, 643 (2010).
[8] D. Yamamoto, G. Marmorini, and I. Danshita, Phys. Rev. Lett. **112**, 127203 (2014).
[9] T. Ono, H. Tanaka, H. Aruga Katori, F. Ishikawa, H. Mitamura, and T. Goto, Phys. Rev. B **67**, 104431 (2003).
[10] N. A. Fortune, S. T. Hannahs, Y. Yoshida, T. E. Sherline, T. Ono, H. Tanaka, and Y. Takano, Phys. Rev. Lett. **102**, 257201 (2009).
[11] C. Griset, S. Head, J. Alicea, and O. A. Starykh, Phys. Rev. B **84**, 245108 (2011).
[12] Y. Shirata, H. Tanaka, A. Matsuo, and K. Kindo, Phys. Rev. Lett. **108**, 057205 (2012).

[13] H. D. Zhou, C. Xu, A. M. Hallas, H. J. Silverstein, C. R. Wiebe, I. Umegaki, J. Q. Yan, T. P. Murphy, J.-H. Park, Y. Qiu, J. R. D. Copley, J. S. Gardner, and Y. Takano, Phys. Rev. Lett. **109**, 267206 (2012).
[14] T. Susuki, N. Kurita, T. Tanaka, H. Nojiri, A. Matsuo, K. Kindo, and H. Tanaka, Phys. Rev. Lett. **110**, 267201 (2013).
[15] K. Naruse, T. Kawamata, M. Ohno, Y. Matsuoka, H. Sudo, H. Nagasawa, Y. Hagiya, T. Sasaki, and Y. Koike, J. Phys.: Conf. Ser. **568**, 042014 (2014).
[16] D. Yamamoto, G. Marmorini, and I. Danshita, Phys. Rev. Lett. **114**, 027201 (2015).
[17] G. Koutroulakis, T. Zhou, Y. Kamiya, J. D. Thompson, H. D. Zhou, C. D. Batista, and S. E. Brown, Phys. Rev. B **91**, 024410 (2015).
[18] G. Quirion, M. Lapointe-Major, M. Poirier, J. A. Quilliam, Z. L. Dun, and H. D. Zhou, Phys. Rev. B **92**, 014414 (2015).
[19] A. Sera, Y. Kousaka, J. Akimitsu, M. Sera, T. Kawamata, Y. Koike, and K. Inoue, Phys. Rev. B **94**, 214408 (2016).
[20] Y. Kamiya, L. Ge, T. Hong, Y. Qui, D. L. Quintero-Castro, H. B. Cao, M. Matsuda, C. D. Batista, M. Mourigal, H. D. Zhou, and J. Ma, arXiv:1701.07971.
[21] M. Motokawa, Annual Meeting of Physical Society of Japan (1978) (unpublished).
[22] H. Nojiri, Y. Tokunaga, and M. Motokawa, J. Phys. (Paris) **49**, Suppl. C8, 1459 (1988).
[23] T. Nikuni and H. Shiba, J. Phys. Soc. Jpn. **62**, 3268 (1993).
[24] N. Achiwa, J. Phys. Soc. Jpn. **27**, 561 (1969).
[25] C. J. Croese, J. C. M. Tindemans-van Eyndhoven, and W. J. A. Masakant, Solid State Commun. **9**, 1707 (1971).
[26] S. Hirotsu, J. Phys. C **10**, 967 (1977).
[27] K. Adachi, N. Achiwa, and M. Mekata, J. Phys. Soc. Jpn. **49**, 545 (1980).
[28] H. Hyodo, K. Iio, and K. Nagata, J. Phys. Soc. Jpn. **50**, 1545 (1981).
[29] Y. Tazuke, H. Tanaka, K. Iio, and K. Nagata, J. Phys. Soc. Jpn. **50**, 3919 (1981).
[30] H. Tanaka, U. Shotte, and K. D. Shotte, J. Phys. Soc. Jpn. **61**, 1344 (1992).
[31] M. Hiroi, M. Sera, H. Nojiri, N. Kobayashi, M. Motokawa, and H. Tanaka, Physica B **284**, 1605 (2000).
[32] R. Bügel, A. Faißt, H. v. Löhneysen, J. Wosnitza, and U. Shotte, Phys. Rev. B **65**, 052402 (2001).
[33] M. Mino, K. Ubukata, T. Bokui, M. Arai, H. Tanaka, and M. Motokawa, Physica B **201**, 213 (1994).
[34] H. Nojiri, K. Takahashi, T. Fukuda, M. Fujita, M. Arai, and M. Motokawa, Physica B **241**, 210 (1998).
[35] N. Stusser, U. Shotte, A. Hoser, M. Meschke, M. Meissner, and J. Wosnitza, J. Phys.: Condens. Matter **14**, 5161 (2002).
[36] A. E. Jacobs, T. Nikuni, and H. Shiba, J. Phys. Soc. Jpn. **62**, 4066 (1993).
[37] T. Nikuni and A. E. Jacobs, Phys. Rev. B **57**, 5205 (1998).
[38] N. Stusser and R. Sadykov, Experimental Reports, BENSC (2004); N. Stusser, R. Sadykov, and A. Hoser, Experimental Report, BENSC (2005).
[39] Y. Kousaka, H. Ohsumi, T. Komesu, T. Arima, M. Takata, S. Sakai, M. Akita, K. Inoue, T. Yokobori, Y. Nakano, E. Kaya, and J. Akimitsu, J. Phys. Soc. Jpn. **78**, 123601 (2009).
[40] A. Miyake, J. Shibuya, M. Akaki, H. Tanaka, and M. Tokunaga, Phys. Rev. B **92**, 100406(R) (2015).
[41] K. Kawamata, H. Sudo, Y. Matsuoka, K. Naruse, M. Ohno, T. Sakai, and Y. Koike, J. Phys.: Conf. Ser. **568**, 042013 (2014).
[42] A. G. Christy, R. J. Angel, J. Haines, and S. M. Clark, J. Phys.: Condens. Matter **6**, 3125 (1994).
[43] Y. Uwatoko, T. Hotta, E. Matsuoka, H. Mori, T. Oki, J. L. Sarrao, J. D. Thompson, N. Mori, and G. Oomi, Rev. High Pressure Sci. Technol. **7**, 1508 (1998).
[44] M. Sera, N. Sato, and T. Kasuya, J. Phys. Soc. Jpn. **57**, 1412 (1988).
[45] T. Nikuni and H. Shiba, J. Phys. Soc. Jpn. **64**, 3471 (1995).
[46] G. Marmorini, D. Yamamoto, and I. Danshita, Phys. Rev. B **93**, 224402 (2016).